VAISHAKHA PUBLICATIONS

Journal of Radiation, Environment and Climate

journal homepage: https://vaishakha.com/index.php/jrec

JOURNAL OF RADIATION, ENVIRONMENT & CLIMATE

Structure studies of Californium isotopes $^{200-300}$Cf

Ummukulsu E.*, Vibha C. P., Shamil Mohammed

Department of Physics, Farook College (Autonomous), Kozhikode, 673632

Abstract—The study of nuclear structure plays an important role in understanding the properties and stability of heavy elements. This work presents a theoretical study on the structural properties of californium (Cf) isotopes in the mass number range 200–300. The Dirac-Hartree-Bogoliubov (DIRHB) model, which offers a self-consistent description of nuclear structure, is used to conduct the analysis within the framework of relativistic mean-field theory. Through important nuclear parameters such binding energy per nucleon, charge radius, root mean square (RMS) radius, two-neutron separation energy, and quadrupole deformation parameter (β_2), the study aims to comprehend the behavior of heavy nuclei. The study examines how nuclear structure changes as the number of neutrons increases and finds patterns in nuclear stability, deformation, and shell effects. The results obtained from this study provide important findings into the structural characteristics of Californium isotopes, mainly in regions where experimental data is limited or unavailable. This work advances our knowledge of nuclear structure in the actinide area and demonstrates how well the DIRHB model describes the characteristics of heavy nuclei. The findings also help extend the nuclear landscape for californium isotopes and provide a basis for future theoretical and experimental studies in nuclear physics. The present work confirm the possibility of having shell closure or midshell closure at N=138.

Keywords: *Californium isotopes; DIRHB Model; nuclear structure; quadrupole deformation; shell closure; Binding energy.*

Received 14 June 2026; **Revised** 18 July 2026; **Accepted** 25 July 2026; **Available online** 15 Aug 2016

1. INTRODUCTION

The study of nuclear structure is essential for understanding the stability, shape, and properties of atomic nuclei especially in the region of heavy and super-heavy elements. To study these complex system accurately, advanced theoretical models and computational methods are needed, one of the widely used approaches is the relativistic self-consistent mean field framework, which provides reliable description of nuclear properties across the entire nuclear chart. In this work, we have chosen to focus on the heavy nucleus of Californium. Californium is a synthetic (man-made) element and belongs to the actinide series in the periodic table. This element has a very large and unstable nucleus, containing a high number of protons and neutrons, which makes it highly radioactive. By using californium as a case study, this work connects theoretical concepts of heavy element formation with a real example of a heavy nucleus. The study of nuclear structure, particularly for heavy and superheavy elements, is essential for understanding the fundamental properties of atomic nuclei. Heavy nuclei show complicated behaviors like deformation, pairing correlations, and shell effects. These behaviors are very important for figuring out their stability and structure. Elements like Californium, belonging to the actinide series, are more importance due to their large mass number and significant applications in nuclear science and technology. Many studies have focused on understanding their physical, chemical, and nuclear properties [1], [2], [3]. The understanding of nuclear structure has been significantly improved by theoretical models, particularly mean-field methods, which play a crucial role in its study. The Hartree-Fock-Bogoliubov (HFB) framework has therefore been established for explorations of ground-state properties of nuclei, capturing simultaneously mean-field and pairing correlations. These models incorporate nucleon interactions, pairing effects, and shell corrections, providing a fundamental understanding of nuclear behavior. But as we approach the regime of heavy nuclei, relativistic effects also start to play an important role and relativistic extensions have been developed such as the Relativistic Hartree-Bogoliubov (RHB) model. Experimental studies are limited for many heavy nuclei, especially in unexplored regions so theoretical models are essential for predicting their structural properties and behavior. In our previous study we have noticed some peculiar behaviour around neutron number N=138 in thorium isotopes [4]. This study motivate us to check whether this behaviour is observed in other actinides also. Here we have considered only few structural behavior of Californium isotopes.

*Corresponding author.

E-mail address: ummukulsu.e@gmail.com (Dr. E. Ummukulsu)

2. THEORETICAL FORMALISM

Mean field theory is one of the most important approaches used to describe the structure of atomic nuclei. In nuclear physics, the many-body problem (many nucleons interacting) is very complex. Mean field theory simplifies this by assuming: Each nucleon moves independently in an average potential (mean field) created by all other nucleons.This converts the problem into a one-body problem, making calculations possible. This approach allows for accurate and computationally feasible descriptions of nuclear properties.

Relativistic Mean Field (RMF) theory is a sophisticated methodology employed to characterize the structure of atomic nuclei, especially heavy nuclei. In this framework, nucleons are regarded as relativistic particles and are characterized by the Dirac equation rather than the Schrödinger equation. The Lagrangian density is the starting point of RMF theory. It shows the system's total energy and includes contributions from free nucleons and their interactions:

$$\mathcal{L} = \mathcal{L}_N + \mathcal{L}_m + \mathcal{L}_{\text{int}}$$

The free nucleon part of the Lagrangian is given by:

$$\mathcal{L}_N = \bar{\psi}\left(i\gamma^\mu \partial_\mu - m\right)\psi$$

with m being the bare mass of a nucleon. $\mathcal{L}_m$ is the Lagrangian of the free meson field and the electromagnetic field.

$$\mathcal{L}_m = \frac{1}{2}\partial_\mu \sigma \partial^\mu \sigma - \frac{1}{2}m_\sigma^2\sigma^2 - \frac{1}{2}\Omega_{\mu\nu}\Omega^{\mu\nu} + \frac{1}{2}m_\omega^2\omega_\mu\omega^\mu - \frac{1}{4}\vec{R}_{\mu\nu}.\vec{R}^{\mu\nu} + \frac{1}{2}m_\rho^2\vec{\rho}_\mu\vec{\rho}^\mu - \frac{1}{4}F_{\mu\nu}F^{\mu\nu} \quad (1)$$

In equations (2) and (3), ψ represents the Dirac-spinors and σ, ω and ρ represent the isoscalar-scalar meson, the isoscalar-vector meson and the isovector-vector meson, respectively. The corresponding masses of these mesons are m_σ, m_ω, and m_ρ and $\Omega_{\mu\nu}, \vec{R}_{\mu\nu}, F^{\mu\nu}$ are the field tensors with,

$$\Omega_{\mu\nu} = \partial_\mu\omega_\nu - \partial_\nu\omega_\mu \quad (2)$$

$$\vec{R}_{\mu\nu} = \partial_\mu\vec{\rho}_\nu - \partial_\nu\vec{\rho}_\mu \quad (3)$$

and

$$F^{\mu\nu} = \partial_\mu A_\nu - \partial_\nu A_\mu \quad (4)$$

The interaction term L_{int} is,

$$L_{int} = -g_\sigma\bar{\psi}\psi\sigma - g_\omega\bar{\psi}\gamma^\mu\psi\omega_\mu - g_\rho\bar{\psi}\vec{\tau}\gamma^\mu\psi\cdot\vec{\rho}_\mu - e\bar{\psi}\gamma^\mu\psi A_\mu \quad (5)$$

with $g_\sigma, g_\omega, g_\rho$ and e being the coupling constants[5]. From this Lagrangian density, the Hamiltonian density was obtained by the Legendre transformation.

$$\mathcal{H}(\mathbf{r}) = \sum_i^A \psi_i^+(\boldsymbol{\alpha}\mathbf{p} + \beta m)\psi_i + \frac{1}{2}[(\nabla\sigma)^2 + m_\sigma^2\sigma^2] - \frac{1}{2}[(\nabla\omega)^2 + m_\omega^2\omega^2] - \frac{1}{2}[(\nabla\rho)^2 + m_\rho^2\rho^2] - \frac{1}{2}(\nabla A)^2 + [g_\sigma\rho_s\sigma + g_\omega j_\mu\omega^\mu + g_\rho\vec{j_\mu}.\vec{\rho}^\mu + e j_{p\mu}A^\mu] \quad (6)$$

Also,

$$\rho_s(\mathbf{r}) = \sum_{i=1}^A \bar{\psi}_i(\mathbf{r})\psi_i(\mathbf{r}), \quad (7)$$

$$j_\mu(\mathbf{r}) = \sum_{i=1}^A \bar{\psi}_i(\mathbf{r})\gamma_\mu\psi_i(\mathbf{r}), \quad (8)$$

$$\vec{j}_\mu(\mathbf{r}) = \sum_{i=1}^A \bar{\psi}_i(\mathbf{r})\vec{\tau}\gamma_\mu\psi_i(\mathbf{r}), \quad (9)$$

$$j_{p\mu}(\mathbf{r}) = \sum_{i=1}^Z \psi_i^+(\mathbf{r})\gamma_\mu\psi_i(\mathbf{r}) \quad (10)$$

Equations 7, 8, 9 and 10 represent entities called the isoscalar-scalar density, isoscalar-vector current, isovector-vector current and electromagnetic current, respectively. Here, the summation index runs over the occupied states in the Fermi sea of positive energy. By integrating equation (8) over the r-space, we obtain the total energy [5] as a function of the meson fields and Dirac spinors. The total energy is,

$$E_{RMF}[\psi, \bar{\psi}, \sigma, \omega^\mu, \rho^\mu, A^\mu] = \int d^3r\mathcal{H}(\mathbf{r}) \quad (11)$$

This basic model, which includes interaction terms that are only linear in the meson fields, does not offer a precise or quantitative description of complex nuclear systems [6, 7]. Hence, it appears more appropriate to adopt the approach proposed by Brockmann and Toki [8], which involves using density-dependent couplings. In this framework, the coupling constants g_σ, g_ω, and g_ρ are considered to be vertex functions associated with Lorentz-scalar bilinear expressions of nucleon operators [5]. In many applications, the couplings between mesons and nucleons depend on the vector density, which can be expressed as $\rho_v = \sqrt{j_\mu j^\mu}$ with the nucleon four-current $j^\mu = \bar{\psi}\gamma^\mu\psi$. In RMF theory, meson fields mediate the interaction between nucleons. Using the mean field approximation, these meson fields are replaced by their average values, which makes the problem much easier to solve. The scalar field creates an attractive force, and the vector field explains the repulsive force inside the nucleus. The mean field approximation applied to the Lagrangian yields the Dirac equation for nucleons in the context of scalar and vector potentials:

$$[-i\boldsymbol{\alpha} \cdot \nabla + \beta (m + S(r)) + V(r)]\, \psi_i = \epsilon_i \psi_i$$

where $S(r)$ is the scalar potential and $V(r)$ is the vector potential. These potentials arise from the interaction terms and depend on the nucleon densities.

The vector potential can be expressed as:

$$V(r) = \alpha_V \rho_v + \alpha_{TV} \tau_3 \rho_{tv} + eA_0 + \sum_R$$

This equation shows how the nuclear mean field is constructed from different density-dependent terms. Thus, RMF theory provides a self-consistent framework for describing nuclear structure by combining relativistic dynamics with mean-field interactions, making it particularly suitable for studying heavy nuclei.

3. RESULTS AND DISCUSSION

We have studied the different structure properties of Californium isotopes from mass number 200 to 300 by using DIRHB code. The structure properties included Binding energy per nucleon, Charge radius, RMS radius, Two neutron separation energy, and Beta deformation parameter.

3.1 Binding Energy

Binding energy of a nucleus is the energy used to bound together the constituents protons and neutrons or it is the energy that we should provide to break the nucleus into nucleons. We have calculated the binding energy per nucleon for even-even nuclei of Californium isotopes in a range of mass numbers 200 to 300 using . The output relativistic mean field theory. The obtained data are compared with the reference data and they are in good match with it [9]. The graph of binding energy per nucleon along with some experimental values are given in figure 1. The graph shows a good agreement with the experimental values. The energy first decreases up to a neutron number 138, the minimum value is shown at the neutron number 142 and then starts to increase slowly up to N=160 and then increases gradually. The increase in binding energy per nucleus shows, how strongly the nucleons are bounded within the nucleus or how much energy we should apply to separate one nucleon, more the binding energy, more stable. Thus from this observation, we can assume that the region N=138 (A=234) to N=160 (A=258) is a valley of stability. Also this is the region that includes in the nuclear landscape chart. But at N=138, an unusual bump can be seen , which indicate the sudden shape transition.

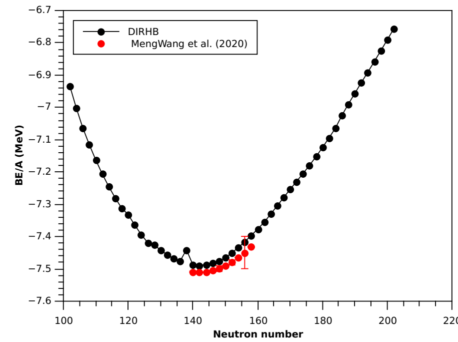

Figure 1: Variation of Binding energy per nucleon with Neutron number of $^{200-300}Cf$ obtained from DIRHB and compared with available data [9]

3.2 Charge Radius

Charge radius is the distance from the center of nucleus to the proton clouds inside the nucleus. It helps to understand the spacial distribution of positive charge inside the nucleus. For heavier nuclei, as it has not a spherical shape. The charge radius for spherical symmetry can be calculated by the equation

$$\langle r^2 \rangle_p = \frac{\int_0^\infty \rho_p(r)\, r^4\, 4\pi\, dr}{\int_0^\infty \rho_p(r)\, r^2\, 4\pi\, dr} \tag{12}$$

Where, ρ_p(r)= Charge density distribution.
$\langle r^2 \rangle$= Mean square charge radius, representing the average of the squared distance from the center.

$$r_{\mathrm{ch}} = \sqrt{\langle r^2 \rangle_p} \tag{13}$$

Generally for all shapes including spherical and deformed shapes we can calculate charge radius by the equation:

$$r_{\mathrm{ch}} = \sqrt{\langle r^2 \rangle_p + r_p^2} \tag{14}$$

The charge radius explains how is the distribution of protons inside a nucleus [10].

We have calculated the charge radius for even-even nuclei of Californium isotopes in a range of mass numbers 200 to 300 and output is plotted in graph Figure 2. The obtained data are compared with the reference data and they are in good match with it [11, 12]. The graph shows an increase in radius with respect to the neutron number. It is not a linear increase in the beginning i.e, from the neutron number 100 to 138. after 138, the curve is almost linearly increasing and almost matches with the experimental data. As the number of neutrons increases, the nuclear size increases, so radius also increases, but here we should consider deformations also. At the points N=126, and 184, the nucleus appear a spherical shape because 126 is magic number where shell closure attains and 184 is a centre of island of stability, the experimental results are still out of reach but reliable theoretical prediction are crucial for directing [13]. In the region N=100 to 118, the energy is increasing slowly. At a region 120 to 126, a sudden drop because of the shell closure at 126. Nucleons become more tightly bound so charge radius will be small. From 128 to 136, a gradual increase in energy occur because of starting of deformation again after the spherical shape, but the sudden dip at 138 shows the stability by attaining spherical shape again. This is also clear from its beta two values.

At the region, $N \approx$140 to 155 another theoretical data (red coloured) shows a large deviation. This data is calculated from the experimental α-decay energies and half life using a theoretical framework based on WKB (Wentzel-Kramers-Brillouin), GDDCM (Generalized density dependent cluster model) models [12]. So it is an indirect calculation, and if the half lives and decay energies have significant uncertainties, the resulting charge radii exhibit large deviation. But DIRHB calculations are direct calculations so will be more accurate.

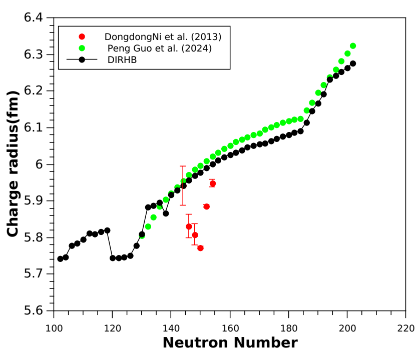

Figure 2: Variation of charge radii of Californium isotopes with neutron numbers and compared with the data of [11, 12]

3.3 RMS Radius

The total root mean square radius of a nucleus describes the average spacial extention of nucleons. The total root mean square (RMS) radius of a nucleus is defined as:

$$r_{\rm rms} = \sqrt{\langle r^2 \rangle} \tag{15}$$

where

$$\langle r^2 \rangle = \frac{1}{A} \int r^2 \rho(r)\, d^3 r \tag{16}$$

$$r^2_{\rm rms} = \frac{Z}{A} r_p^2 + \frac{N}{A} r_n^2 \tag{17}$$

A: Total number of nucleons (mass number), equal to $Z + N$.
r: Distance of a nucleon from the center of the nucleus.
$\rho(r)$: Total matter density distribution (protons and neutrons).

Here we are calculating total rms radius, so that the shape and properties of nuclei can analyse as it gives the true size of the nucleus. In heavy nucleus the neutron distribution dominates the growth so neutron rms radius will be greater than that of proton and thus the total rms radius will increase.

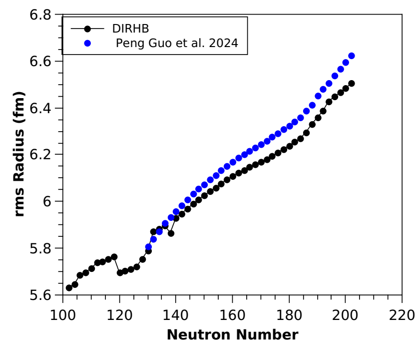

Figure 3: Variation of rms radii of Californium isotopes with the neutron number and compared with [11]

We have calculated the rms radius for even-even nuclei of Californium in a range of mass numbers 200 to 300 using the DIRHB code. The output data is plotted in figure 3. The obtained data are compared with the reference data and they are in good match with it [11]. The rms radius curve is almost similar to the charge radii curve. It also show totally an increase with respect to the increase in neutron number as physically expected. But it shows good agreement with the reference values. In the region N=118 to 126 a sudden dip and a small flattened region is visible it is because of the shell closure at the magic number 126. And the density distribution will be more compact.

From 130 to 136, a small increase due to starting of deformation again and a sudden dip at the N=138, which again says about a shell closure or midshell closure at 138, like in the charge radius graph. After N=160, the graph shows a steady increase, no sharp shape transitions. From this graph, we get that at small neutron numbers, nucleons occupy at discrete energy levels and the shell effects are high. But as the nuclei become bigger and bigger, shell effects less dominate, neutron distribution spreads out more so radius starts increase faster. At higher neutron numbers the behaviour is like liquid drop model. The small deviation at 138 arises because, the data in blue color is taken from mass table by Peng Guo et al.[11], in which they uses different density functional PC-PK1, but in our calculation we used the density functional DD-PC1.

3.4 Separation energy

The separation energy is very important quantity that measures the energy required to remove a single nucleon or a group of nucleons from a nucleus. It provide an idea of binding energy and the structure of nuclear energy levels. Separation energy is directly related to the binding energy. It is mainly used to study about decay processes and other nuclear reactions and the nuclear properties like shape especially for heavy nuclei. Separation energies define the ultimate limits of nuclear existence. For most stable nuclei, separation energies are roughly 6-10 MeV. The neutron separation energy is the energy required to remove one neutron from the nucleus S_n. The proton separation energy is lower compared to the neutron separation energy, this is because of the repulsive force between the protons. S_p and S_n will become zero at proton and neutron driplines respectively. The difference in binding energy of adjacent nuclei gives separation energy this is explained by the equations

$$S_n(Z,N) = B(Z,N) - B(Z,N-1) \tag{18}$$

$$S_p(Z,N) = B(Z,N) - B(Z-1,N) \tag{19}$$

The two neutron separation energy is the energy needed to remove 2 neutrons from the nucleus. The nucleons have tendency to form pairs. So More separation energy is required to remove nucleon from an even-even nuclei than an even-odd, or odd-odd nuclei.

We have calculated the two neutron separation energy for even-even nuclei of Californium isotopes in a range of mass numbers 200 to 300 and graph is plotted in figure 4. The obtained data are compared with the reference data [11] and they are in good match with it. In this graph we can see a total increase of the separation energy as neutron number increases which matches with the physical theory, as the neutron increases, the shells in which they have to be filled will be less tightly bound. So the neutron separation energy will decrease. In the graph, it is negative values hence shows an increasing trend. A significant variation is seen at neutron numbers N= 138. Throughout the isotopic evolution, the shape of nuclei varies between prolate and spherical shapes. The sudden bumps in the graph is because of attaining stability by the nucleus at or about that neutron number, the high peaks may indicates a sudden change from highly deformed shape to stable spherical or vice versa. The region 126 is well known magic number, so the shape of nucleus become spherical and become more stable so the energy needed to remove two neutron will increase. The nucleus may highly deformed and becoming stable spherical shape at the points N= 138, that may the reason for the sharp transition, also it is supported from the binding energy per nucleon graph, as the S_2n values are calculated from that. Next bump can be seen at 184, which is also a region of stability [1], [13]that is nucleus approaches spherical shape.

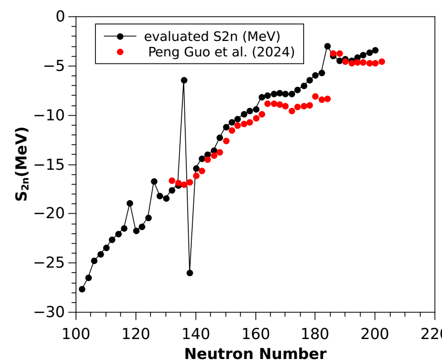

Figure 4: Variation of two neutron separation energy of californium isotopes with neutron number and compared with the reference data [11]

3.5 Quadrupole Deformation Parameter β_2

It is a numerical quantity that describes the degree of deformation from the spherical shape. This Quadrupole deformation occurs only when the valence shell is unfilled. The equation connecting β_2 and reduced transition probability is.

$$\beta_2 = \frac{4\pi}{3ZR^2}\left[B(E2)\uparrow \frac{e^2b^2}{e^2}\right]^{1/2} \tag{20}$$

where, R is the average radius

$$R = R_0 A^{1/3} \tag{21}$$

where, $\quad R_0 = 1.2 fm$

The equation connecting quadrupole moment and reduced transition probability is

$$Q_0 = \left[\left(\frac{16\pi}{5}\right)\frac{B(E2)e^2b^2}{e^2}\right]^{1/2} \tag{22}$$

An equation connecting quadrupole moment and β_2

$$Q_0 = \left(\frac{16\pi}{5}\right)^{1/2}\beta_2\frac{3ZR^2}{4\pi} \tag{23}$$

The deformation parameter β_2 has different ranges over different shapes. When its value is less than 0 ($\beta_2 < 0$) the nuclear shape will be oblate. When it is equal to zero ($\beta_2 = 0$) the shape is spherical. when it is greater than 0 ($\beta_2 > 0$), the shape is prolate.

We have calculated the β_2 deformation parameter for even-even nuclei of Californium in a range of mass numbers 200 to 300 using the DIRHB code. The output graph is plotted in figure 5. The obtained data are compared with the reference data [14, 15, 16] and they are in good match with it. The values of β_2 deformation parameters are directly taken from the output of the code, and it gives a direct relation to the shape of nuclei. From the obtained values, we can understand that, the Californium nuclei are prolate and spherical shaped. The graph shows strong deformation at low neutron number sudden drops at certain values in the middle and another sudden dip at the neutron number 184. From N $\approx$ 100 to 116 β_2 is large and nuclei are strongly prolate. May be the arrangement of charged protons within the nucleus with less neutron number and trying to reduce maximum repulsive force between them is leading to this shape. The nuclei are far from closed shells, many valence nucleons has strong quadrupole correlations and leads to collective rotational motion. From a region N$\approx$ 118 to 126 the $\beta_2 \approx 0$, as we know 126 is magic number, so there attains a shell closure. From 128 to 136, again the shape is deformed, it may be because of the valence neutron starts filling in higher orbitals. A sudden drop is there at 138, which indicates a shell closure or shape transition. Between 140 and 160, a moderate stable deformation can be seen. It is not near shell closure, but almost a stable deformation. By looking at the values of β_2, from 168 to 192 the shape is almost spherical and there may be a strong shell closure at 184, hence the dip. From that, deformation again starts and from 1994 to 202, the shape is again prolate, hence a gradual increase in that region.

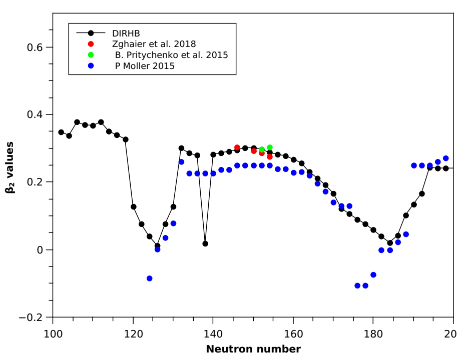

Figure 5: variation of β_2 values of Californium isotopes with neutron number and compared with the reference data [14, 15, 16]

4. CONCLUSION

In the present work , we explore the nuclear structure properties of californium isotopes in the mass number range 200 to 300. The primary objective was to analyse how important nuclear parameters such as binding energy per nucleon, charge radius, root mean square (RMS) radius, two-neutron separation energy, and quadrupole deformation parameter (β_2) vary with neutron number and to identify the variation around neutron number N=138. These nuclear properties were evaluated using a relativistic mean-field framework based on the Dirac-Hartree-Bogoliubov (DIRHB) model, which provides a self-consistent description of mean-field and pairing correlations in heavy nuclei. The results were obtained and analyzed separately for each isotope, and the corresponding graphs were plotted to study the variation of nuclear properties. The selection of the isotopic range was guided by the nuclear landscape, allowing the study to extend into neutron-rich regions where experimental data is limited and nuclei are highly unstable. Due to the scarcity of experimental information for many of these isotopes, a direct comparison with experimental results was not always possible. Instead, the focus was placed on systematically analyzing and interpreting the predicted values obtained from the DIRHB model. For validation and reliability, available experimental and theoretical data from published literature were used for comparison wherever possible. A key aspect of this study was to investigate the evolution of nuclear structure properties with neutron number. For each parameter—particularly binding energy per nucleon, charge radius, RMS radius, two-neutron separation energy, and quadrupole deformation parameter (β_2)—the results were carefully analyzed to understand trends related to nuclear stability, shell effects, and shape transitions. In conclusion, it can be stated that the role of shell effects and nuclear deformation in affecting some important nuclear properties has been clearly demonstrated by this study using a large number of Californium isotopes. We have observed that interesting behavior in californium isotopes also. So this study also evident for shell closure or midshell closure at neutron number N=138.

Acknowledgement

I would like to express my sincere thanks to department of physics, Farook college for providing computing facilities.

References

[1] E. M. Holmbeck, T. M. Sprouse, and M. R. Mumpower, “Nucleosynthesis and observation of the heaviest elements,” *The European Physical Journal A*, vol. 59, no. 2, p. 28, 2023.

[2] C. J. Hansen, “Heavy elements: They came out of the blue,” *Experimental astronomy*, vol. 55, no. 1, pp. 133–147, 2023.

[3] R. G. Haire, “Californium,” in *The chemistry of the Actinide and Transactinide elements*, pp. 1499–1576, Springer, 2011.

[4] E. Ummukulsu and A. Joseph, “Investigation on the structure properties of thorium nuclei spanned between the drip-lines and the prediction of shell closure,” *The European Physical Journal Plus*, vol. 138, no. 12, p. 1077, 2023.

[5] T. Nikšić, N. Paar, D. Vretenar, and P. Ring *Computer Physics Communications*, vol. 185, no. 6, pp. 1808–1821, 2014.

[6] J. Boguta and A. Bodmer, “Relativistic calculation of nuclear matter and the nuclear surface,” *Nuclear Physics A*, vol. 292, no. 3, pp. 413–428, 1977.

[7] W. Pannert, P. Ring, and J. Boguta, “Relativistic mean-field theory and nuclear deformation,” *Physical Review Letters*, vol. 59, no. 21, p. 2420, 1987.

[8] R. Brockmann and H. Toki, “Relativistic density-dependent hartree approach for finite nuclei,” *Physical Review Letters*, vol. 68, no. 23, p. 3408, 1992.

[9] M. Wang, W. J. Huang, F. G. Kondev, G. Audi, and S. Naimi, “The ame 2020 atomic mass evaluation (ii). tables, graphs and references,” *Chinese Physics C*, vol. 45, no. 3, p. 030003, 2021.

[10] I. Sick, “Proton charge radius from electron scattering,” *Atoms*, vol. 6, no. 1, 2018.

[11] P. Guo, X. Cao, K. Chen, Z. Chen, M.-K. Cheoun, Y.-B. Choi, P. C. Lam, W. Deng, J. Dong, P. Du, *et al.*, “Nuclear mass table in deformed relativistic hartree–bogoliubov theory in continuum, ii: Even-z nuclei,” *Atomic Data and Nuclear Data Tables*, vol. 158, p. 101661, 2024.

[12] D. Ni, Z. Ren, T. Dong, and Y. Qian, “Nuclear charge radii of heavy and superheavy nuclei from the experimental α-decay energies and half-lives,” *Physical Review C—Nuclear Physics*, vol. 87, no. 2, p. 024310, 2013.

[13] E. M. Ramirez, D. Ackermann, K. Blaum, M. Block, C. Droese, C. E. Düllmann, M. Dworschak, M. Eibach, S. Eliseev, E. Haettner, *et al.*, “Direct mapping of nuclear shell effects in the heaviest elements,” *Science*, vol. 337, no. 6099, pp. 1207–1210, 2012.

[14] H. A. Zghaier, S. A. Ebrahiem, and H. Abdul_Jabbar, “Study the shapes of nuclei for heavy elements with mass number equal to ($226 \leq a \leq 252$) through determination of deformation parameters for two elements (u&cf),” *Ibn AL-Haitham Journal For Pure and Applied Science*, vol. 31, no. 3, pp. 10–19, 2018.

[15] B. Pritychenko, M. Birch, B. Singh, and M. Horoi, “Tables of e2 transition probabilities from the first 2+ states in even–even nuclei,” *Atomic Data and Nuclear Data Tables*, vol. 107, pp. 1–139, 2016.

[16] P. Möller, A. J. Sierk, T. Ichikawa, and H. Sagawa, “Nuclear ground-state masses and deformations: Frdm (2012),” *Atomic Data and Nuclear Data Tables*, vol. 109, pp. 1–204, 2016.